

ROLLOVER CRASHES: DIVING VERSUS ROOF CRUSH

Raphael Grzebieta

David Young

Michael Bambach

Department of Civil Engineering, Monash University, Australia

Andrew McIntosh

School of Safety Science, The University of New South Wales, Australia

Paper Number: 07-0394

ABSTRACT

A rational analysis of the two apparently conflicting views of neck injury causation for contained and belted occupants in rollover crashes that have been presented in research literature to date, i.e. torso augmentation (diving) vs. roof intrusion, is presented. The validity of each of the views and associated injury causation mechanisms and underlying concepts are investigated using basic Newtonian laws of physics.

Through the analysis of General Motors Malibu II rollover test series, the authors show how roof crush at high intrusion velocities results in high neck loading. Equations are developed that demonstrate how roof intrusion is integrally linked to neck loading and hence is the main causal factor of serious neck injuries in rollover crashes. The paper also shows how roof intrusion compounds torso augmentation resulting from rollover kinematic motion.

Discussions are also presented regarding the “lift shaft” analogy proposed by Moffatt and used to explain how serious head and neck injuries occur in rollover crashes. The authors show that analogy is inappropriate by at least an order of magnitude in terms of the crash severity it suggests.

INTRODUCTION

31,041 passenger vehicle occupants were killed in the US in 2005 of which 10,608 died in crashes where their vehicle rolled over [1]. This includes passenger car, pickups, utilities & vans. **Figure 1** shows that there has been a steady rise in such fatalities over the past decade despite the introduction of a number of injury mitigation initiatives by NHTSA. In contrast, **Figure 1** indicates non-rollover related vehicle occupant fatalities have been steadily declining.

The most likely reason for the downward trend in non-rollover related crash fatalities is vehicles are

subjected to both government and consumer dynamic crash testing using Anthropomorphic crash Test Dummies (ATD) for both frontal offset and side impact crashes. There is no equivalent mandated or consumer dynamic crash test being carried out to rate vehicle rollover crashworthiness. There only exists a mandated quasi-static test FMVSS216 [2]. This test has been shown to be ineffective in protecting occupants in real world rollover crashes by a number of researchers and professionals concerned about rollover crashworthiness [3, 4, 5].

It will be interesting to monitor over the next five or so years whether rollover related fatalities will decrease as a result of the introduction of electronic stability control. In the mean time it is clear there must a considerable ramping of effort to enhance the roll-over crashworthiness of vehicles. This paper deals with a number of the issues currently being debated in the US concerning vehicle rollover crashes.

Injuries to seat belted occupants involved in rollover crashes were investigated by the authors in preceding papers [5, 6]. A number of issues relating to the debate concerning whether injuries result from diving or roof intrusion were discussed and the GM rollover Malibu II test series were analysed. This paper further elaborates on some of the issues discussed and presents additional analysis of some of the Malibu II test series.

DIVING MECHANISM

In an attempt to explain why injuries were occurring in vehicle rollover crashes, Moffatt proposed in 1975 that such injuries resulted from a mechanism analogous to diving. He argued that when the roof contacts the ground, it can be considered to be stationary against it, with the body of the car and the occupant continuing to move towards, and eventually striking, the

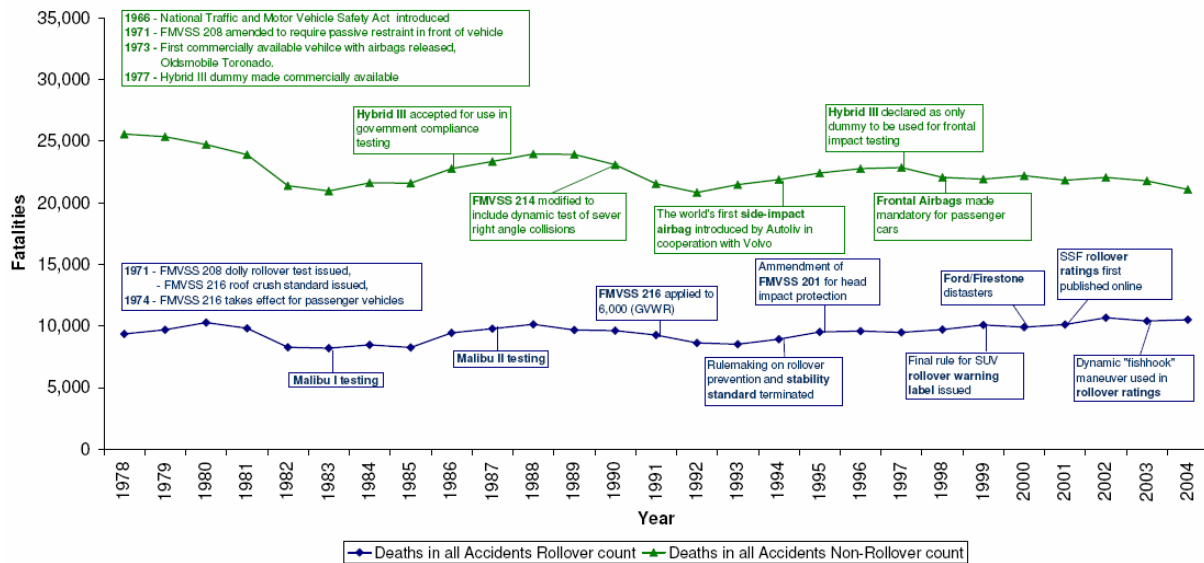


Figure 1: US Rollover related vehicle fatalities compared to all other vehicle crash fatalities.

ground/roof surface. The injury mechanism resulting from this strike was likened to the neck injury that occurs when a person dives into shallow water in a pool, river or lake.

Moffatt also contended that the injuries were not causally related to the roof intrusion, i.e.

“When the roof of the vehicle struck the ground, it essentially came to rest relative to the ground. The roof struck the ground and stopped, but the body of the vehicle continued to move towards the roof.”

Evolving from this rationalisation of how rollover injuries occur was the concept of torso augmentation. In other words, when an occupant’s head stops against the roof of the vehicle during a roof to ground impact, the torso of the occupant continues to move towards the roof/ground at the same rate as the vehicle is approaching towards the ground. The occupant’s neck and head is thus loaded, resulting in head, neck and spinal injuries. Moffatt drew an analogy between the injury mechanism he described that occurs in a rollover crash to one that would occur to a person inside a lift where a cable brakes resulting in the lift falling down a lift shaft as depicted in his sketch in **Figure 2**. He further elaborated:

“The occupant continues to fall until he strikes the floor of the elevator, which has stopped at the bottom of the elevator shaft.... The higher fall caused the increased injuries, and the higher fall caused the increased crush to the sides of the elevator”

The authors discussed this issue in a previous paper [6]. However this analogy requires further

analysis. The elevator shaft defence has been used consistently by industry since 1975 to aid in product litigation related to injuries to contained occupants resulting from rollover crashes where there is evidence of significant roof intrusion.

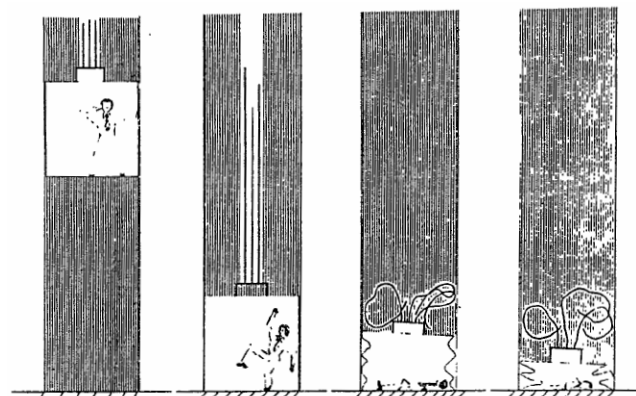


Figure 2 – Copy of Figures 11a to 11d “lift-shaft” analogy presented by Moffatt [8].

The image shown in **Figure 2** indicates a lift dropping approximately 3 stories in a lift well, i.e. around 6 metres. In contrast, Friedman and Nash (2005) on analysing GM rollover Malibu II test data found that

“The center of gravity of a rolling vehicle does not rise or fall more than a few inches during a rollover. Thus, the vertical velocity of the centre of gravity of the vehicle at roof impact is low – virtually never more than 2.5 m/sec (5 mph).”

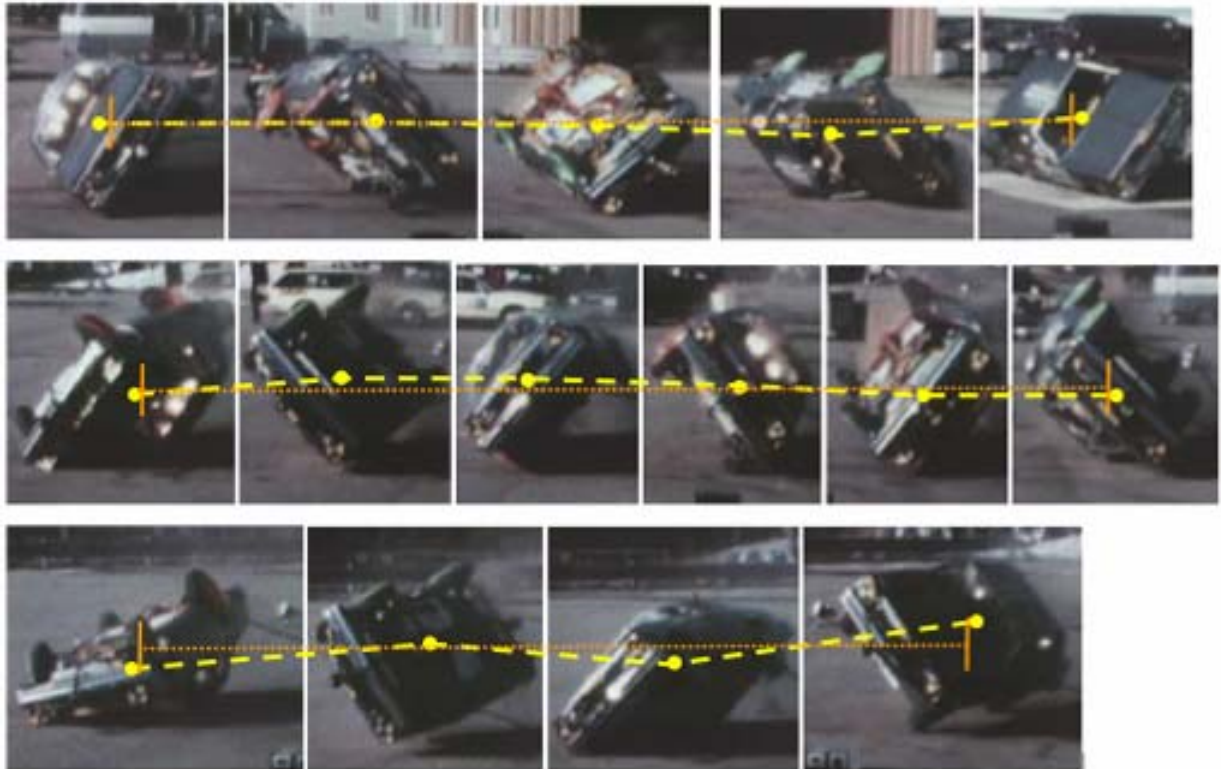


Figure 3: Frame sequence from GM rollover Malibu II test number 7 showing how the height of the vehicle's COG does not vary significantly during the rollover event.

Figure 3 shows how the height of the Centre of Gravity (COG) varies over the duration of a FMVSS 208 rollover crash test. The frames were obtained from a high speed film of GM's Malibu II test number 7. It was in this particular test that the highest neck loading of 13,200 N on the driver (7L4) was recorded [6, 9]. The orange end bars shown in **Figure 3** represent a length of approximately 61 cm (2 ft). The 7L4 neck loading occurred 3.787 seconds into the test when the vehicle roof contacted the ground. This also happened to be the last quarter turn of the crash event (last two frames in **Figure 3**).

If the falling lift analogy proposed by Moffatt is adopted, it would appear that the vertical drop height observed in the last two frames of **Figure 3** would be around 30.5 cm (1 ft). The vertical velocity from rotation was around 1.9 m/sec (Young et al [6]) Using Newtonian laws of physics, the velocity 'v' the vehicle could reach if it were to drop through such a height 'h' would be around

$$v = \sqrt{2gh} + 1.9 \quad \dots (1)$$

$$= \sqrt{2 \times 9.81 \times 0.0305} + 1.9 \approx 2.7 \text{ m/sec}$$

or around 9.6 km/hr or 6.0 mph. This is a very low impact velocity.

Carrying out the same calculations for a lift dropping through 6 metres as depicted by Moffatt in **Figure 2**, the impact velocity reached by the lift just prior to impact would be around 10.8 m/sec (39 km/hr or 24 mph). Hence, Moffatt's "lift shaft" analogy grossly over estimates the severity of the rollover event by at least one order of magnitude. It thus presents an inaccurate representation of the roof crush and subsequent injury process.

A question that is worth considering when contemplating Moffatt's "lift shaft" analogy, is what engineering changes would need to be carried out on the lift that would allow the person inside to survive such a 6 metre drop. One only needs to visualise the image of the lift shaft with the lift replaced by a car attached inside as shown in **Figure 4**. With the occupant held in the seat with a tensioned harness belt, it becomes obvious that the 6 meter fall is readily survivable. Indeed at a crash speed of 39 km/hr the occupant would most likely walk away from the fall.

Another way the Moffatt "lift shaft" scenario can be visualised as survivable is to place an air cushion at the bottom of the lift shaft. The cushion would decelerate the lift at a uniform rate of deceleration. Accepting that a person can survive a deceleration of around 10 g's it is possible to estimate the

distance over which the lift would need to be decelerated in order for the person inside to survive. The fundamental equation that governs the behaviour of all decelerating objects is

$$v^2 = 2as \quad \dots (2)$$

where 'a' is the deceleration and 's' is the distance over which the body is decelerated. Thus the thickness of the air cushion would need to be

$$s = \frac{v^2}{2a} = \frac{10.8^2}{2 \times 10 \times 9.81} \approx 0.6 \text{ m}$$

Thus to decelerate the lift so that the person inside survives with no or minor injury from which he/she can recover, an air cushion of only 0.6 metres would be required as shown in **Figure 5**.



Figure 4: Car hung in lift shaft with occupant strapped into tensioned seat belt.

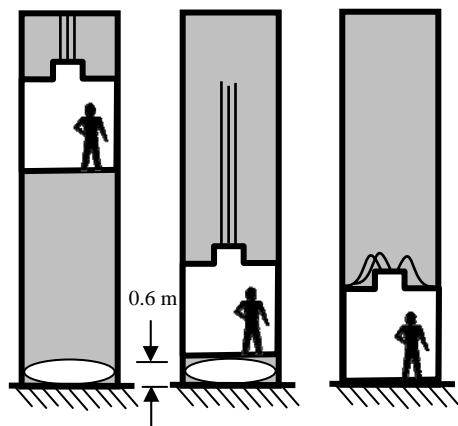


Figure 5 Energy absorber at base of lift that decelerates lift falling from 3 stories to 10 g's.

Note that equation (2) is independent of mass. This means equation (2) can be used to determine what minimum distance is required to slow a vehicle down and its occupants restrained inside so that they do not suffer a major injury. This equation was

formulated in the early nineteenth century, i.e. almost 200 years ago.

Of course, because the severity of rollovers is an order of magnitude less than the lift falling three floors, the distance required to safely decelerate an occupant within the vehicle that has a strong roof structure will be accordingly far less. Nevertheless, what is more important to realise is that the deformation mechanism proposed by Moffatt in **Figure 2** bears no comparison to a 'real world' crash test shown in **Figure 3**.

To try to understand how non-ejected seat belted occupants are injured in rollover crashes, the authors have focussed on further analysing the results of the General Motors (GM) Malibu II rollover crash tests.

MALIBU II CRASH TESTS & ROOF STRIKE

GM undertook a series of FMVSS 208 dolly rollover crash tests of their 1983 Chevrolet Malibu vehicle, with seat belted occupants, in 1987. The series is referred to as the Malibu II rollover crash tests. Eight vehicles were tested. Four vehicles had roofs strengthened with a 'roll cage' and four 'production' vehicles had no strengthening. The Hybrid III 50th percentile ATD's were restrained with the vehicle's seatbelt systems. The belts were fitted to the ATD's with slack equivalent to the static inversion of a human surrogate in the vehicle. The rollover crashworthiness performance of the strengthened roll cage vehicles was compared to the production vehicles by Bahling et al [10].

ATD neck loads were measured. Any neck load above 2000 N was identified as a Potentially Injurious Impact (PII). There were forty (40) such PII's recorded from the test series. **Figure 6** shows a graph of the PII's recorded [6] where it has been noted whether or not the PII was during roof-to-ground contact.

The authors have discussed the maximum PII load 7L4 recorded in test number 7 in a prior paper [6]. This paper looks in more detail at neck loads 3L2 and 3L3 and the associated roof deformation mechanisms.

Slow motion film recordings of test number 3 were investigated in detail. Reference lines were drawn along the top of the seat back and vertical from the seat back to the middle of the rear view mirror as shown in **Figure 7**. The length of a line drawn from the horizontal and vertical reference lines to an identifiable point on the roof at the B-pillar (roof deformation) and to the ATD's head (head movement) as well as the length of a line from the

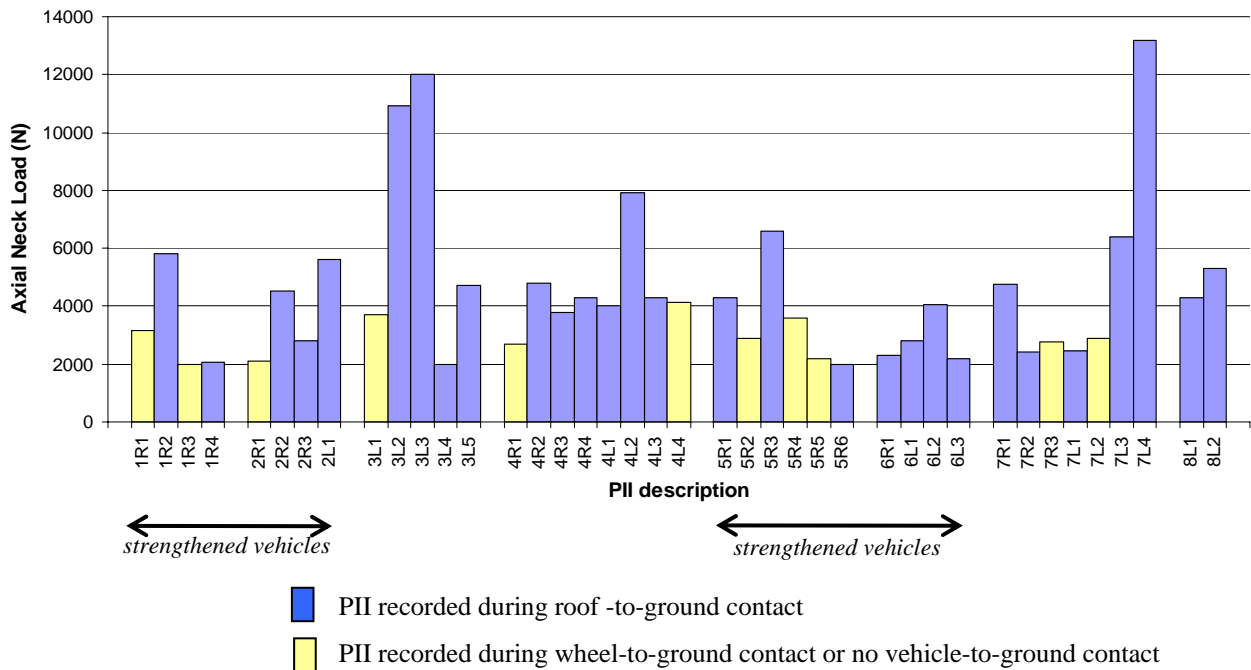


Figure 6: - Malibu II PII axial neck loads

head to the ATD’s shoulders (neck compression) was measured in each of the 3 millisecond frames for neck loads 3L2 and 3L3. The data obtained is plotted in **Figures 8 & 9**. Whilst the values obtained are only as accurate as can be measured from each high speed film frame, they do provide a basis on which an understanding can be reached of how the load is applied to the ATD’s neck during a rollover crash.

It is clear that in PII 3L2 the neck load occurs at the moment where the slope of the roof displacement versus time curve rises rapidly as indicated in **Figure 8 (b)**, i.e. where the vertical roof intrusion velocity is at its highest. What is interesting to note is the horizontal displacement is approximately twice the magnitude of the vertical displacement (**Figure 8 (a)**). Taking into account both vertical and horizontal displacement the resultant roof intrusion velocity at the moment 3L2 was recorded is around 5 m/sec (18 km/h or 11.2 mph).

Another interesting point to note from **Figure 8 (c)** is the ATD’s shoulder does not move relative to the seat back until well after the neck had been loaded, i.e. at 625 ms. Once the load is imparted onto the ATD’s head from the intruding roof, the neck is compressed as a result of the torso’s inertia preventing it from immediately moving in unison with the roof crush and head. The shoulder starts to move at 625 ms and eventually catches up with the forced displacement (roof & head movement).

Figure 9 shows the comparable graphs for PII 3L3. Similar characteristics can be noted here as well, i.e.

- the horizontal deformation is around twice the vertical deformation
- the roof intrusion velocity relative to the seat back and torso is again around 5 m/sec (18 km/h or 11.2 mph)
- the torso begins to move well after the neck has been loaded and then unloaded
- the head movement is closely coupled to the roof intrusion

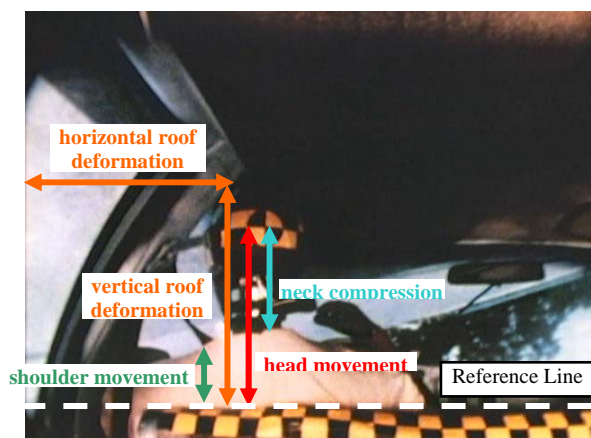
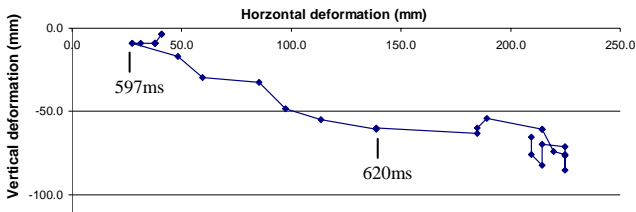
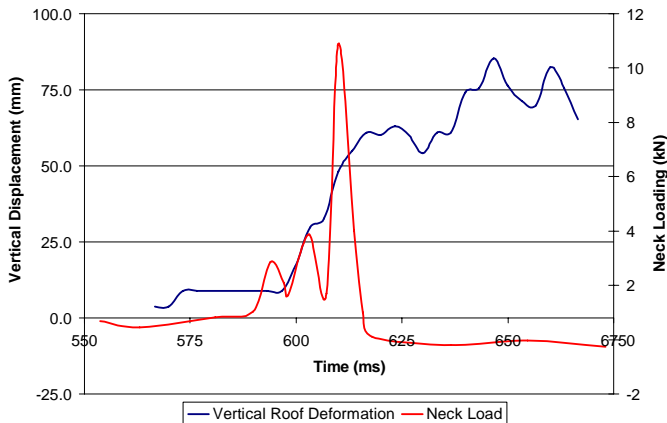


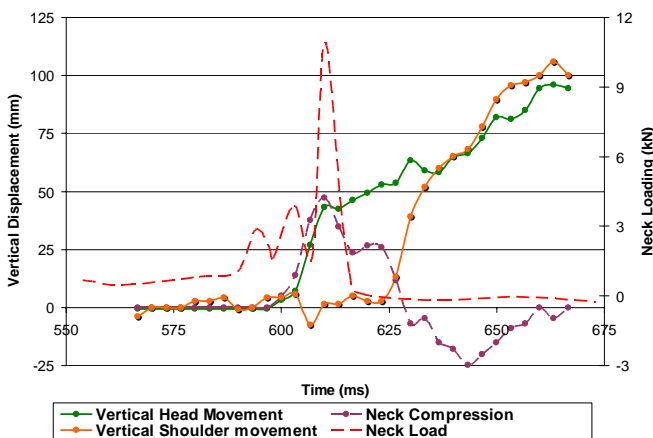
Figure 7 Lines measured during each 3 millisecond frame.



(a) PII: 3L2 Horizontal versus vertical roof deformation



(b) PII: 3L2 Vertical roof deformation and neck load versus time.



(c) PII: 3L2 Vertical head & shoulder movement and neck compression versus time compared to neck loading versus time.

Figure 8: Vehicle roof crush & ATD neck loading, head movement, shoulder movement & neck compression for Malibu II 2L2.

This is a similar result to that obtained by Friedman and Nash [9] for the 3L3 PII though the magnitude of roof crush appears to be different. The main reason for this is that only the vertical displacement is graphed in **Figure 8** whereas it is not clear what measure was used by Friedman and Nash [9] to plot roof crush. From the high speed films it appears the B-pillar and A-Pillar intrude a considerable distance sideways into the occupant compartment.

It is worth noting that Friedman and Nash [9] calculated a value of 10.1 mph for the B-pillar intrusion. This confirms the accuracy of the value calculated is reasonable considering the methodology chosen to obtain the graphs shown in **Figures 8 & 9**. Indeed, frame images from Malibu test 3 confirm the torso moves after the neck has been compressed as shown in **Figures 10 & 11**. In PII 3L2 compression is predominantly axial whereas in PII 3L3 the neck loading appears to be subjected to combined axial and shear.

The torso moves somewhat similar as would a single degree of freedom mass reacting against a compressed spring at one end and then pulling on the spring subjecting the neck to tension (**Figures 8(c) & 9(c)**).

In regards to the Moffatt [8] diving analogy, i.e. when the vehicle's roof contacts the ground, the occupant's head stops against the roof, and then the torso of the occupant and vehicle (visualise bench seat back in **Figures 11 & 12**) continues to move towards the roof/ground at the same rate, it appears at first glance that the information in **Figures 7, 8, 11 & 12** confirms the mechanism he proposed. However, to better understand what is actually occurring in terms of the head-torso interaction with the vehicle roof and the issue of diving versus roof crush, a mathematical model characterising the occupant dynamics and neck loading needs to be considered. Such a model was proposed and analysed by the authors in a previous paper [6]. The analysis of that model is extended further here.

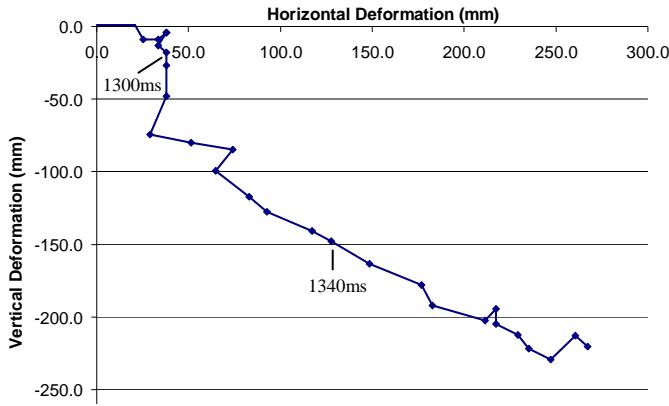
NECK-TORSO SIMPLIFIED MODEL

Figure 10 shows two simplified single degree of freedom dynamic models representing the Hybrid III dummy's torso, neck and head shown in **Figures 11 & 12**. There are three possible scenarios in which the neck in this model can be loaded; **Figure 10 (a)** Roof crush; **Figure 10 (b)** Diving; and a combination of diving and roof crush.

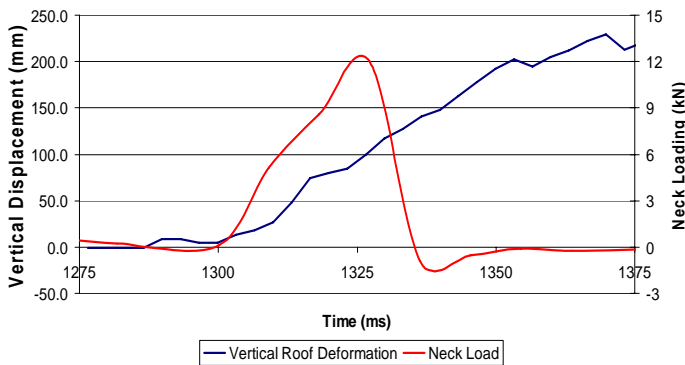
To analyse this model, the following simplifying assumptions must be made first namely:

- All movement of the head and/or torso is absorbed through compression of the neck. In other words, the torso-neck-head interaction is a single degree of freedom system subjected to an imposed vertical motion. The motion is applied as a result of either the roof striking the head and moving the head towards the torso or the torso mass moving at a constant velocity towards a rigid surface roof/ground.
- No damping of the force occurs due to impact with the head.

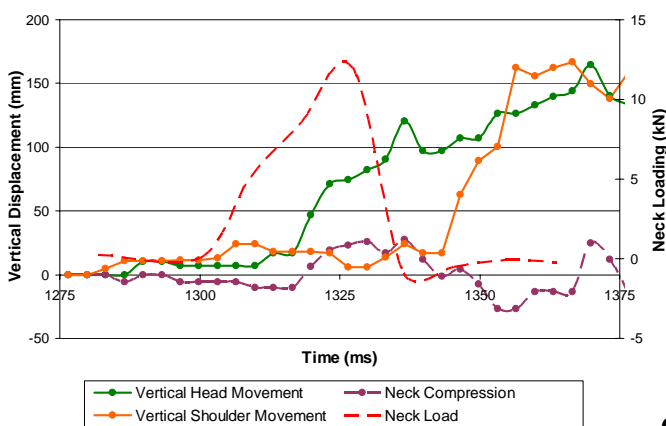
- As is suggested in Moffatt's diving theory all loading on the neck is produced by the inertia of the dummy's torso (torso augmentation).
- Deceleration/acceleration occurs at a constant rate.



(a) PII: 3L3 Horizontal versus vertical roof deformation



(b) PII: 3L3 Vertical roof deformation and neck load versus time.



(c) PII: 3L3 Vertical head & shoulder movement and neck compression versus time compared to neck loading versus time.

Figure 9: Vehicle roof crush & ATD neck loading, head movement, shoulder movement & neck compression for Malibu II 3L3.

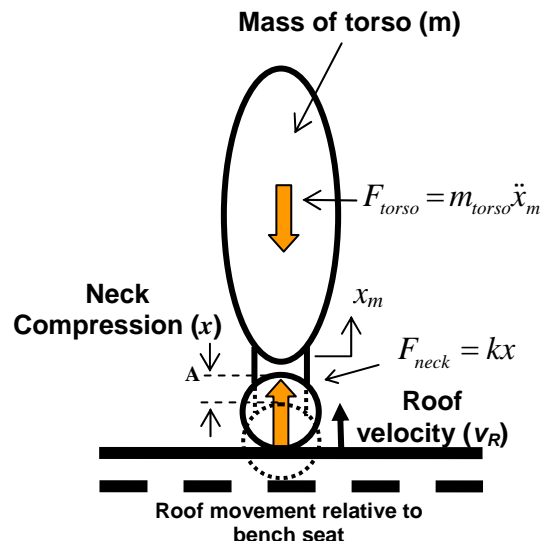
- Force is constant throughout the neck, i.e. same force at the top of the neck, C1 position, and the base of the neck, C7 position.
- The head and neck stay aligned as shown in **Figure 10** for the duration of loading, resulting in a purely compressive load.

Roof Crush:

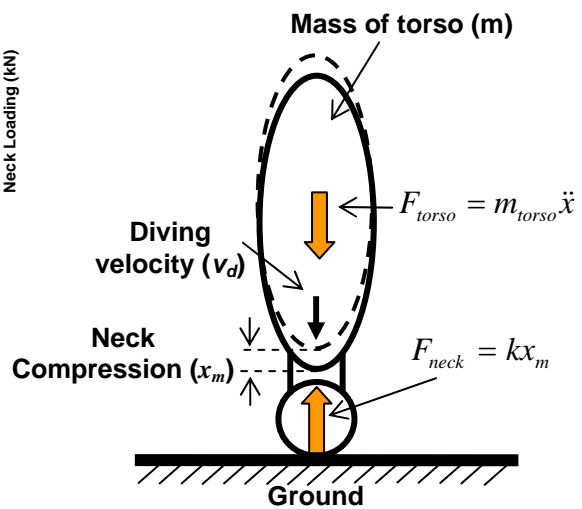
Using **Figure 10 (b)** the equation of motion, i.e. equilibrium of mass at any instant is

$$k(x - x_m) = m\ddot{x}_m \quad \dots (3)$$

where k is the ATD's neck stiffness, x the neck compression, x_m the displacement of the torso, m



(a) Roof crush



(b) Diving

Figure 10: Single degree of freedom dynamic model representing Hybrid III dummy



Head under side rail near B-pillar. Note three neck rings visible.



Neck compressed. Note only two neck rings visible and sensor cable flatter.



Torso now moving and three neck rings just visible. B-pillar has move laterally inwards.



Torso moved lower relative to seat back. Neck is now longer.

Figure 11: Kinematics of PII 3L2



Head under side rail near B-pillar. Note three neck rings visible.



Neck compressed and head moved side ways. Note small "v" in T-shirt neck line left of centreline of head when compared to frame above.



Torso now starting to catch up with neck and head



Torso moved lower and across relative to seat back.

Figure 12: Kinematics of PII 3L3

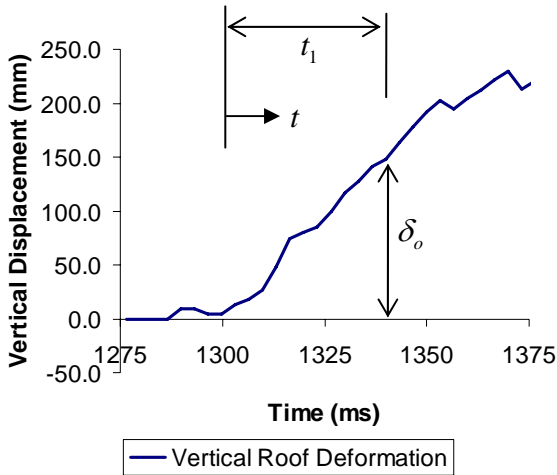


Figure 13: Roof crush versus time from PII 3L3.

the mass of the torso and \ddot{x}_m the acceleration of the torso. Thus the governing dynamic equation is

$$m\ddot{x}_m + kx_m = kx \quad \dots (4)$$

Roof crush appears to linearly vary with time as indicated in **Figure 13**. Hence,

$$x = \delta_0 \frac{t}{t_1} \quad \dots (5)$$

where t is the time from the start of neck loading, t_1 is the time over which neck loading occurs and δ_0 is the magnitude of displacement at the end of the loading phase. Thus substituting into right hand side of Equation (4)

$$m\ddot{x}_m + kx_m = k\delta_0 \frac{t}{t_1} \quad \dots (6)$$

Equation (6) is a well known 2nd order non-homogenous differential equation with constant coefficients. It's solution is composed of a general solution being the complimentary solution x_c and the particular solution x_p . Thus

$$x_c = A \sin \omega t + B \cos \omega t \quad \dots (7)$$

where A and B are integration constants and

$$\omega = \sqrt{\frac{k}{m}} \quad \dots (8)$$

is the circular frequency.

The displacement during the phase over which loading occurs (t_1) can be determined using

Equation (5). The particular solution for this loading is

$$x_p = \delta_0 \left(\frac{t}{t_1} \right) \quad \dots (9)$$

Thus the full solution for the movement of the torso is

$$x_m = x_c + x_p = A \sin \omega t + B \cos \omega t + \delta_0 \left(\frac{t}{t_1} \right) \quad \dots (10)$$

and its velocity is

$$\dot{x}_m = A \omega \cos \omega t - B \omega \sin \omega t + \frac{\delta_0}{t_1} \quad \dots (11)$$

and its acceleration

$$\ddot{x}_m = -A \omega^2 \sin \omega t - B \omega^2 \cos \omega t \quad \dots (12)$$

From initial conditions we know that at $t = 0$ the torso has not moved and thus its displacement is assumed to be zero, i.e. $x_m = 0$. Thus using Equation (10)

$$A \sin(\omega \times 0) + B \cos(\omega \times 0) + \delta_0 \left(\frac{0}{t_1} \right) = B = 0 \quad \dots (13)$$

and also at $t = 0$ the velocity of the torso is assumed to be zero, i.e. $\dot{x}_m = 0$. Hence substituting into Equation (11) results in

$$A = -\frac{\delta_0}{\omega t_1} \quad \dots (14)$$

Thus substitution and rearranging terms the displacement of the torso for the loading phase when the roof is crushing is

$$x_m = \frac{\delta_0}{t_1} \left(t - \frac{\sin \omega t}{\omega} \right) \quad \dots (15)$$

and its velocity is thus

$$\dot{x}_m = \frac{\delta_0}{t_1} (1 - \cos \omega t) \quad \dots (16)$$

and its acceleration

$$\ddot{x}_m = \frac{\delta_0 \omega}{t_1} \sin \omega t \quad \dots (17)$$

From **Figure 10 (a)** the load in the neck of the ATD can be expressed as

$$F_{neck} = k(x - x_m) \quad \dots (18)$$

Hence using Equation (15) and Equation (5)

$$F_{neck} = kx - k \frac{\delta_0}{t_1} \left(t - \frac{\sin \varpi t}{\varpi} \right) = k \frac{\delta_0 t}{t_1} - k \frac{\delta_0}{t_1} \left(t - \frac{\sin \varpi t}{\varpi} \right) \quad \dots (19)$$

which simplifies to

$$F_{neck} = \frac{k \delta_0}{t_1} \frac{\sin \varpi t}{\varpi} = \frac{\sqrt{km} \delta_0 \sin \varpi t}{t_1} \quad \dots (20)$$

Using Equation (5), the velocity at the interface between the head and the neck (point A in **Figure 10 (a)**) is

$$\dot{x} = \frac{\delta_0}{t_1} \quad \dots (21)$$

thus

$$F_{neck} = \dot{x} \sqrt{km} \sin \varpi t$$

The load varies over time. This means that the load in the dummy's neck is largest when

$$\frac{\partial F_{neck}}{\partial t} = 0 = \ddot{x} \sqrt{km} \varpi \cos \varpi t$$

Thus when the acceleration is zero the neck loading is a maximum and when $\cos \varpi t = 0$, $\varpi t = \frac{\pi}{2}$.

Substituting this and Equation (21) into

Equation (20) results in $F_{neck} = \dot{x} \sqrt{km} \sin \frac{\pi}{2}$ and

when simplified and replacing the term $\dot{x} \equiv V_R$ is

$$\boxed{F_{neck} = V_R \sqrt{km}} \quad \dots (22)$$

Thus knowing the velocity of the roof crush, the stiffness of the ATD's neck and the mass of the torso, the peak axial force in the neck can be determined.

Diving:

To determine what the neck load would be in the situation where the torso and head move towards the ground the model in **Figure 10 (b)** is now considered. In this instance equilibrium of forces at any instant is

$$kx_m = m\ddot{x}_m \quad \dots (23)$$

resulting in the following governing equation

$$m\ddot{x}_m + kx_m = 0 \quad \dots (24)$$

Equation (24) is a 2nd order homogenous differential equation with constant coefficients.

The solution to **Equation (24)** is the same as the general solution for a single degree of freedom mass subjected to undamped vibration, i.e. Equations (7) & (8). Thus the velocity in this instance is

$$\dot{x}_m = A \varpi \cos \varpi t - B \varpi \sin \varpi t \quad \dots (25)$$

and acceleration is the same as Equation (12).

From initial conditions at $t = 0$ the displacement of the torso is assumed to be zero, i.e. $x_m = 0$.

Thus using Equation (7)

$$A \sin(\varpi \times 0) + B \cos(\varpi \times 0) = B = 0 \quad \dots (26)$$

and also at $t = 0$ the velocity of the torso is assumed to be constant during neck loading, i.e.

$\dot{x}_m = v_d$ (see Figure 12 in Young et al [6]). Hence substituting into Equation (7)

$$A \varpi \cos(\varpi \times 0) - 0 = A \varpi = v_d \quad \dots (27)$$

resulting in

$$A = \frac{v_d}{\varpi} \quad \dots (28)$$

Thus the final governing equations for the loading phase when the torso and neck are diving into the roof/ground is

$$x_m = \frac{v_d}{\varpi} \sin \varpi t \quad \dots (29)$$

and the velocity is thus

$$\dot{x}_m = v_d \cos \varpi t \quad \dots (30)$$

and acceleration

$$\ddot{x}_m = -v_d \varpi \sin \varpi t \quad \dots (31)$$

From **Figure 10 (b)** the load in the neck of the dummy is expressed as

$$F_{neck} = k x_m \quad \dots (32)$$

Hence using Equation (29)

$$F_{neck} = k \frac{v_d}{\varpi} \sin \varpi t \quad \dots (33)$$

which can also be expressed as

$$F_{neck} = v_d \sqrt{km} \sin \varpi t \quad \dots (34)$$

The load varies over time. This means that the load in the dummy's neck is largest when

$$\frac{\partial F_{neck}}{\partial t} = 0 = v_d \sqrt{km} \varpi \cos \varpi t = k v_d \cos \varpi t$$

$$\text{This means } \varpi t = \frac{\pi}{2} \text{ or } t = \frac{\pi}{2\varpi} = \frac{\pi}{2} \sqrt{\frac{m}{k}}$$

Thus substituting into Equation (34) for ϖt

$$\boxed{F_{neck} = v_d \sqrt{km}} \quad \dots (35)$$

This is exactly the same equation as Equation (22), i.e. there is no mathematical difference between roof crush and diving from an engineering dynamics perspective.

Combined roof crush and diving:

In this instance the roof is crushing in at a velocity of v_R as shown in **Figure 10 (a)** while at the same time the torso is moving towards the incoming roof at v_d as shown in **Figure 10 (b)**. In this case the equilibrium of forces is the same as for roof crush alone, i.e. Equation (3). Thus the governing equation is Equation (4).

Roof crush will still vary linearly during the load phase. Hence Equation (5) is still valid for the neck compression and Equation (6) is the governing dynamic equation. The solution to this equation is represented by Equations (10), (11) and (12). However this is where the mathematical similarity to roof crush ends.

The initial conditions are different in this case, i.e. at $t = 0$ the displacement of the torso is adopted as zero such that $x_m = 0$. Thus using Equation (12)

$$A \sin(\varpi \times 0) + B \cos(\varpi \times 0) + \delta_0 \left(\frac{0}{t_1} \right) = B = 0 \quad \dots (36)$$

but at $t = 0$ the velocity of the torso is constant, i.e. $\dot{x}_m = v_d$. Hence substituting into Equation (11)

$$A \varpi \cos(\varpi \times 0) - 0 + \frac{\delta_0}{t_1} = A \varpi + \frac{\delta_0}{t_1} = v_d \quad \dots (37)$$

resulting in

$$A = \frac{1}{\varpi} \left(v_d - \frac{\delta_0}{t_1} \right) \quad \dots (38)$$

Therefore the dynamic equations for the loading phase when the roof is crushing towards the occupant and the occupant is diving into the roof is

$$x_m = \frac{1}{\varpi} \left(v_d - \frac{\delta_0}{t_1} \right) \sin \varpi t + \delta_0 \left(\frac{t}{t_1} \right)$$

and after rearranging terms is

$$x_m = \frac{v_d}{\varpi} + \frac{\delta_0}{t_1} \left(t - \frac{\sin \varpi t}{\varpi} \right) \quad \dots (39)$$

and the velocity is the same as Equation (16) and acceleration is the same as Equation (17)

The load in the neck of the dummy is the same as Equation (18). Hence using Equation (39) and Equation (5)

$$\begin{aligned} F_{neck} &= kx - k \left[\frac{v_d}{\varpi} - \frac{\delta_0}{t_1} \left(t - \frac{\sin \varpi t}{\varpi} \right) \right] \\ &= k \frac{\delta_0 t}{t_1} - k \frac{v_d}{\varpi} - k \frac{\delta_0}{t_1} \left(t - \frac{\sin \varpi t}{\varpi} \right) \end{aligned}$$

which simplifies to

$$F_{neck} = k \left(\frac{v_d}{\varpi} + \frac{\delta_0}{t_1} \frac{\sin \varpi t}{\varpi} \right) = \sqrt{km} \left(v_d + \frac{\delta_0 \sin \varpi t}{t_1} \right) \quad \dots (40)$$

From Equation (5) the velocity at the neck head interface is

$$\dot{x} = \frac{\delta_0}{t_1}$$

Thus

$$F_{neck} = \sqrt{km}(v_d + \dot{x} \sin \varpi t) \quad \dots (41)$$

The load varies over time. This means that the load in the dummy's neck is largest when

$$\frac{\partial F_{neck}}{\partial t} = 0 = \dot{x} \sqrt{km} \varpi \cos \varpi t$$

Thus when the acceleration is zero the neck loading is a maximum as all other terms are non-zero regardless of the speed of the torso's initial diving velocity.

Again if $\cos \varpi t = 0$. This means $\varpi t = \frac{\pi}{2}$ or

$$t = \frac{\pi}{2\varpi} = \frac{\pi}{2} \sqrt{\frac{m}{k}}$$

Thus substituting into Equation (41)

$$F_{neck} = \sqrt{km} \left(v_d + \dot{x} \sin \frac{\pi}{2} \right)$$

and finally after replacing the term $\dot{x} \equiv v_R$, results in

$$F_{neck} = \sqrt{km}(v_d + v_R) \quad \dots (46)$$

This means that the roof crush and the diving components combine together resulting in an increase in load to the neck. That this is the case has been shown by the authors in a previous paper for injury 7L4 (Young et al [6]). However, only the diving component of the impact was calculated and shown to be around half the neck load measured where roof crush was evident. Equation (46) shows that the intrusion velocity of the roof needs to be added to the diving velocity of the ATD to obtain the correct value of the neck load.

NECK LOAD CALCULATIONS

To calculate the torso velocity, the high speed film was digitised into single frame images and the rotational and vertical movements for a given time period were noted. The rotational velocity (ω) and vertical velocity (v_v) was calculated. This was then

used to determine the respective rotational and vertical velocity changes of the vehicle where the time period was started when the driver's side or passenger side roof rail touched the ground until the peak neck load was observed. The period was around 20 - 40 ms.

The equivalent change in tangential velocity (Δv_ω) the dummy would be subjected to as a result of rotation was determined using the position of the dummy and the rotational velocity change of the vehicle. The distance from the dummy's COG to the vehicle's COG, which in turn was assumed to be at the centre of rotation, was the lever arm length used to convert rotational velocity. The tangential and vertical velocity changes were then added because both were essentially in the vertical direction (i.e. down) at the time of roof to ground contact. Thus the overall vertical velocity change Δv_d that the dummy's torso would be travelling at was calculated.

Finally, using Equation (35) and the calculated velocities, the theoretical neck load in the case of torso augmentation ("diving") was estimated. **Table 1** shows the rotational, vertical and total (equivalent "diving") velocity change for each vehicle and the resulting theoretical neck load that could be expected as a result of this torso movement. The final column in **Table 1** lists whether the calculated loads minus the measured loads were within estimated calculation errors.

It is clear that using the velocity from rotation and vertical drop only (**Figure 3**), where there is significant roof intrusion (3L2, 3L3 & 4L7), results in an underestimate of the neck load measured in the ATD.

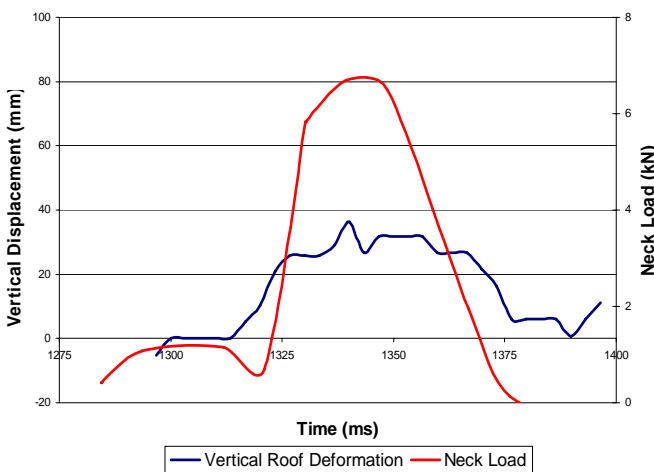
When Equation (22) and the intrusion velocity for 3L2 and 3L3 of 5 m/sec is used, a neck load value of around 12 kN is obtained compared to measured values of 10.9 kN and 12 kN respectively. A neck stiffness of 3.36 kN/cm and a torso mass of 17.19 kg were used to calculate these values (Young et al [6]). The calculated neck loads are within measurement tolerance. Hence this confirms that the neck load is closely coupled with the roof intrusion.

Figurers 8 & 9 show that the torso is not moving relative to the seat back until after the neck load has peaked. The captured images in **Figures 11 & 12** demonstrate that the torso only begins to move well after the neck has been loaded and then unloads.

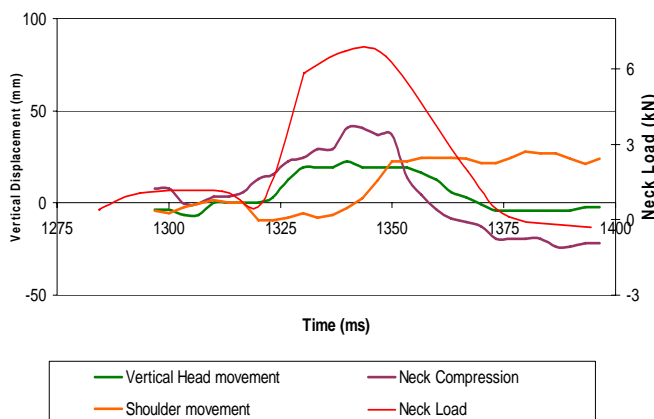
When injury 5R3 is considered, being the highest neck load for a reinforced vehicle, measurements of shoulder and head movements shown in **Figure 14** indicate the ATD's shoulder is moving earlier and

Test	Roof Support	Injury	Position	$\Delta\omega$ (rad/Sec)	Lever arm to COG (m)	ΔV_ω (m/sec)	ΔV_v (m/sec)	ΔV_d (m/sec)	Theoretical Load (N)	Hybrid III Load (N)	Difference (N)	Inside errors?
2	Reinforced	2L1	Far-side	2.4±0.2	0.46	-1.1±0.1	-1.3±0.9	2.4±1.0	5,700±2,400	5,600	-100	Yes
5	Reinforced	5R3	Near-side	1.4±0.3	0.65	-0.9±0.2	-1.7±1.2	2.6±1.4	6,200±3,300	6,600	400	Yes
3	Production	3L2	Far-side	2.6±0.1	0.56	-1.6±0.1	-1.1±1.5	2.7±1.6	6,400±3,800	10,900	-4,500	No
3	Production	3L3	Far-side	2.6±0.1	0.53	-1.3±0.1	-0.5±1.3	1.8±1.4	4,400±3,300	12,000	-7,600	No
4	Production	4L2	Far-side	2.6±0.3	0.69	-1.8±0.2	-0.7±1.2	2.5±1.4	5,900±3,300	7,900	-2,000	Yes
7	Production	7L4	Far-side	2.9±0.2	0.63	-1.9±0.1	-0.9±0.9	2.8±1.0	6,700±2,400	13,200	-6,500	No

Table 1: Theoretical ATD neck loads calculated using Equation (35) compared to measured loads.



(a) PII: 5R3 Vertical roof deformation and neck load versus time.



(b) PII: 5R3 Vertical head & shoulder movement and neck compression versus time compared to neck loading versus time.

Figure 14: ATD neck loading, head movement, shoulder movement & neck compression for Malibu II 5R3.

within the neck loading phase. Hence in this test, neck compression appears to be resulting from a component attributed to torso movement within the reinforced vehicle. Moreover, when the internal views of the ATD for each of the PII's are viewed for the reinforced vehicles, the footage shows the roof and roll cage moving relative to the seat back. **Figure 14 (a)** clearly shows the reinforced roof moving 35 mm vertically downwards relative to the vehicle's seat back. The intrusion velocity is around 2.5 m/sec. Using Equation (22) a value of around 6 kN neck load is obtained. Thus, some form of small roof intrusion is still occurring albeit small and can be observed for most of the PII injuries in the reinforced vehicles.

All of the Malibu II film footage of the reinforced vehicles was also carefully investigated to identify if a PII injury measure existed where there was clearly no roof deformation but torso augmentation was clearly visible. **Figures 15 & 16** show that injury 6L2 matches such a characteristic. **Figure 16** shows the torso moving towards the roof during a near-side impact and no roof deformation on the far-side above the dummy could be perceived in the film. The measurement of the movement of the roof relative to the seat back is graphed in **Figure 15**. It deformed only a few millimetres. The measured neck loading resulting from this diving mechanism, characterised in **Figure 10 (b)**, is graphed in **Figure 15**. The velocity of the torso just prior to the neck being loaded was of the order of 1.7 m/sec. Again using Equation (35) a value for the neck load of around 4 kN is obtained.

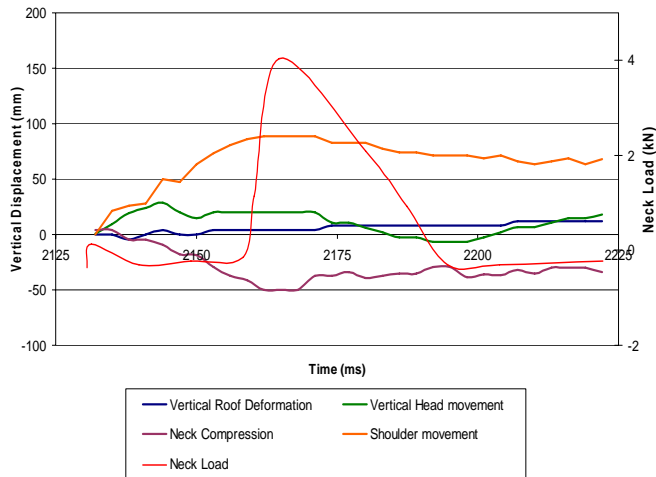


Figure 15 ATD neck loading, head movement, shoulder movement & neck compression for Malibu II 6L2.

CONCLUSIONS

The following conclusions were reached on the basis of the work presented in this thesis.

The “lift shaft” analogy used by Moffatt [8] to describe how injuries occur in rollover crashes does not reflect the measured injuries in real world FMVSS 208 dolly rollover crash tests nor for that matter real world crashes. The magnitude of injury severity in a rollover would be inaccurate by at least an order of magnitude compared to the severity of a lift dropping 3 stories down a shaft and crashing. Similarly, the kinematics of a rollover crash are not comparable to the kinematics of a lift dropping three stories down a lift shaft.

Dissipating the kinetic energy of a lift dropping down a lift shaft three stories in order to prevent anyone inside the lift being injured, only requires an aircushion approximately 0.6 metres deep.

Because the severity of a rollover crash is an order of magnitude less severe than a lift falling three stories, a much smaller energy dissipater such as padding or an air curtain is require to mitigate occupant injuries.

Roof crush increases the severity of neck injuries in rollover crashes.

The neck loading is closely coupled to the velocity of the roof intrusion. This can be proven mathematically using Newtonian laws of physics.

Injurious neck loads would be significantly reduced in rollover crashes if vehicles roofs were strengthened to prevent intrusion at critical velocities.



Vehicle just prior to touch down on near side. Note position of torsorelative to seat back.



Torso moves towards roof (diving into roof) during near side touch down resulting in 6L2 injury measure.

Figure 16 Kinematics of PII 6L2.

ACKNOWLEDGEMENTS

The authors would like to thank the Australian Research Council for providing funds to carry out this research. They would also like to thank the Department of Civil Engineering, Monash University for providing a scholarship for the second author.

The authors would especially like to thank Mr. Don Friedman, Mr. Jack Bish, Ms. Suzie Bozzini, and Ms. Cindy Shipp of Xprts LLC for access to the Malibu test series data and discussions relating to US rollover crashes, and Dr. Bertrand Frechede of School of Safety Science in The University of New South Wales regarding biomechanics issues.

REFERENCES

- [1] National Highway Traffic Safety Administration. 2006. Traffic safety facts, 2005. Report no. DOT HS-810-631. Washington, DC: US Department of Transportation.
<http://www-nrd.nhtsa.dot.gov/pdf/nrd-30/NCSA/TSFAnn/TSF2005EE.pdf>

[2] Federal Motor Vehicle Safety Standards, Part 571; Standard 216.

<http://www.fmcsa.dot.gov/rules-regulations/administration/fmcsr/fmcsrruletext.asp?section=571.216>

[3] Friedman D. & Nash C. Advanced Roof Design for Rollover Protection. 17th International Technical Conference on the Enhanced Safety of Vehicles. Amsterdam, The Netherlands, 2001.

[4] Henderson M. and Paine M., Passenger Car Roof Crush Strength Requirements, Federal Office of Road Safety, 1998.

[5] See National Highway Traffic Safety Administration Docket Management System, Docket Number 22143

<http://dms.dot.gov/search/searchFormSimple.cfm>

[6] Young D, Grzebieta R.H., Bambach M., and McIntosh A., Diving vs Roof Intrusion: A Review of Rollover Injury Causation, submitted to International Journal of Crashworthiness, December, 2006.

[7] Young D., Grzebieta R.H., Rechnitzer G., Bambach M. & Richardson S., Rollover Crash safety: Characteristics and issues, Proceedings 5th International Crashworthiness Conference ICRASH2006, Athens, Greece, July 2006.

[8] Moffatt, E.A., Occupant Motion in Rollover Collisions, in 19th Conference of the American Association of Automotive Medicine. 1975: San Diego, California, USA.

[9] Friedman, D. & Nash, C. E. Reducing Rollover Occupant Injuries: How and How Soon. 19th International Conference on the Enhanced Safety of Vehicles. Washington DC, USA, 6 - 9 June 2005

[10] Bahling G. S., Bundorf R. T., and Kaspzyk G. S., Moffatt E. A., Orlowski, K. F., and Stocke, J. E., "Rollovers and Drop Tests- The Influence of Roof Strength on Injury Mechanics Using Belted Dummies," SAE Paper No. 902314, 34th Stapp Car Crash Conference Proceedings, pp. 101-112, 1990.